

SURFACTANT MODIFIED CNT/EPOXY NANOCOMPOSITES FOR IMPROVED MECHANICAL & FUNCTIONAL PROPERTIES

Yan GENG, Ming Yang LIU, Jing LI, Xiao Mei SHI and Jang-Kyo KIM

*Department of Mechanical Engineering, Hong Kong University of Science & Technology
Clear Water Bay, Kowloon, Hong Kong*

ABSTRACT

Surfactant has been successfully applied to enhance the dispersion of carbon nanotubes (CNTs) in polymer for nanocomposite fabrication. CNTs were treated with nonionic surfactant Triton X-100, and its effect on functional, mechanical and thermo-mechanical properties of CNT/epoxy nanocomposites were evaluated. It is shown that the treatment of CNTs with surfactant improved significantly the electrical conductivity of nanocomposites, the improvement being several orders of magnitude especially at CNT contents below 1.0 wt%. The corresponding percolation threshold of nanocomposites was reduced from 0.09 wt% to 0.06 wt%. This ameliorating effect can be attributed to the hydrogen bonding between the CNT surface and epoxy resin, which in turn improved the interfacial adhesion. The hydrocarbon hydrophobic segment of the surfactant interacts with the CNT surface, whereas the oxyethylenated hydrophilic segment interacts with the epoxy. An improved interfacial adhesion between the conducting filler and polymer matrix is essential to eliminating highly electrically resistant micro- and nano-scale voids along the interface. Unlike other types of functionalization techniques, such as chemical grafting of polymer or amino-functionalization, however, the hydrogen bonds between the CNT and Triton had little adverse effects on either the π bond of CNT or the formation of conducting networks.

The mechanical properties of the treated nanocomposites, including fracture toughness, flexural strength and modulus, as well as the thermo-mechanical properties, such as storage modulus and glass transition temperature, were also shown better than the nanocomposites without treatment. Improved CNT dispersion due to the surfactant was mainly responsible for these observations: the surfactant introduced a steric repulsive force between the CNTs, which in turn helped overcome the van der Waals attractive forces between them. The implications of the synergy on improved interfacial adhesion and dispersion provided by the surfactant are discussed.

1. INTRODUCTION

As an effective nanoscale reinforcement, carbon nanotube (CNT) has attracted great interests in the field of conducting nanocomposites. Such nanocomposites possess outstanding mechanical properties, excellent electrical and thermal conductivities, which are considered useful attributes for many applications in the electronics industry [1-3]. However, the high aspect ratio and the flexibilities of CNTs [4] along with van der Waals forces cause CNTs to be severely entangled in close packing upon synthesis [5]. Furthermore, the chemically inert nature of CNT leads to low dispersability in and weak interfacial interactions with polymer matrix.

To improve the disentanglement and dispersion in the matrix, significant research

efforts have been devoted to the modification of CNTs based both on chemical and physical methods, in the past decade. The chemical methods aim at introducing covalent bonding on CNTs through creating functional groups to enhance the wettability and adhesion characteristics. However, there are two major drawbacks in the use of the chemical functionalization: i) most methods are aggressive, especially oxidation process with acids [6,7], and invariably generate structural defects and deteriorate the intrinsic properties of CNTs; ii) although some milder functionalization processes have been developed, such as UV/ozone treatment or plasmas [8,9], and followed by amine [8,10], silane [11], or fluorine treatments [12], the limited active sites in CNTs (mostly at the defects and end caps) may lead to a low efficiency of functionalization, thus hardly altering the dispersability of CNTs in polymer matrix. In contrast, the non-covalent physical treatments, such as application of surfactants [13,14] and polymer wrapping [15,16], are particularly attractive because of the physical adsorption seldom disturbs the inherent π bonds of CNTs and thus the electrical properties [17].

In this paper, we present an approach based on a nonionic surfactant that has been successfully applied to CNT-epoxy nanocomposites. It was shown that nonionic surfactants are suitable for water non-soluble polymers [17]. The mechanism of nonionic surfactants is based on a strong hydrophobic attraction between the solid surface and the tail group of surfactants. Once the adsorption of surfactants on particle surfaces is established, self-assembly of the surfactant molecules into micelles can be achieved above a critical micelle concentration (CMC). Polyoxyethylene octyl phenyl ether (Triton X-100) with the CMC value of 0.2 mM at 25 °C was used as the nonionic surfactant in this study (see the chemical structure in Fig. 1). Generally, the working concentration of Triton X-100 is between 1-5 mM [18]. In this study, two different concentrations of 1 CMC and 10 CMC were chosen to study the effects on electrical conductivity of nanocomposites.

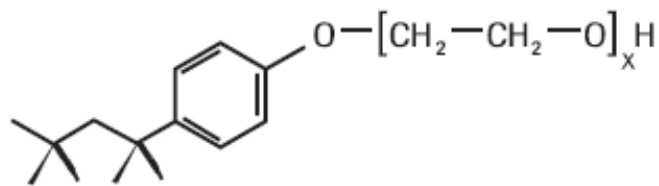


Fig. 1 Chemical structure of Triton X-100 ($x = 9-10$)

2. EXPERIMENTS

2.1 Materials and Fabrication of CNT/epoxy nanocomposites

The multi-wall carbon nanotubes (MWNTs, supplied by Iljin Nanotech, Korea) were produced by a chemical vapor deposition (CVD) method, with the specific surface area of 420 m²/g, the length and diameter ranged 10~15 μ m and 10~20 nm, respectively. Triton X-100 (supplied by VWR International, England) was used as a nonionic surfactant. An epoxy resin, diglycidyl ether of bisphenol A (EPON 828, supplied by Shell Chemical) served as the polymer matrix, and the curing agent was meta-phenylene diamine (mPDA, supplied by DuPont, U.S.). To reduce the entanglement and close

packing, ultrasonication was applied while dispersing CNTs in acetone. Three batches of MWNTs immersed in acetone, namely CNT only, CNT mixed with 1 CMC and 10 CMC surfactants, were subject to ultrasonication for 6 hr at room temperature with a temperature-adjustable sonicator (Branson 1510-DTH).

The as-treated CNT/acetone suspension was poured into epoxy resin and mixed manually to form mixtures with varying CNT contents of 0.025, 0.05, 0.06, 0.08, 0.1, and 0.25 wt%, respectively. The mixture was subject to ultrasonication at 60 °C for 2 hr, followed by degassing in a vacuum oven at 80 °C overnight. The curing agent mPDA was blended with the mixture at a weight ratio of 14.5/100. The composite was moulded into a flat plate, cured at 80 °C for 3 hr and post-cured at 150 °C for 2 hr.

2.2 Characterization

The Fourier transform infrared spectrometry (FTIR, Bio-Rad, FTS 6000) and Raman spectroscopy (Renishaw, RM 3000) were used to identify the surface chemistry of pristine and surfactant treated CNTs. For the FTIR analysis, the CNTs were ground with potassium bromide (KBr) as a diluent and pressed into a pellet. The 514 nm Argon ion laser excitation was used to obtain the Raman spectrum. The dispersion states of CNTs were examined using a transmission electron microscope (TEM, JEOL 2010). The thermomechanical properties of CNT/epoxy nanocomposites were measured on a dynamic mechanical analyzer (DMA 7 Perkin-Elmer), according to the ASTM D4065-90. The samples of 20 mm × 3 mm × 1mm were tested in three point bending at varying temperatures between ambient and 250 °C at a heating rate of 10 °C/min.

The izod impact and flexural tests were performed on neat epoxy and CNT/epoxy nanocomposites according to the ASTM D-256 and ASTM D-790, respectively. Five specimens were tested in each set of condition. The specimens for the impact test were cut into 64 mm × 12.7 mm × 3.2 mm, with a 0.2 mm deep triangular notch at the mid-edge of the specimen. The tests were performed on an impact testing machine (Zwick-Roell HIT515P) with an impactor of 5.5 J. In three-point flexural test, specimens with dimensions of 70 mm × 12.7 mm × 3 mm were loaded in three-point bending until failure with a support span of 50 mm at a constant cross-head speed of 1.3 mm/min on a universal testing machine. The morphologies of fracture surfaces were observed using a scanning electron microscope (SEM, JEOL 6700F).

The bulk electrical conductivity of CNT/epoxy nanocomposites with dimensions of 10 mm × 10 mm × 0.8 mm was measured at room temperature based on the four probe method (Bio-Rad HL5500PC). Regarding the measuring limit of the instrument was up to $10^8 \Omega \text{ cm}$, the samples with electrical resistivity higher than the limit was measured on a programmable curve tracer (Sony Tektronix 370A).

3. RESULTS AND DISCUSSION

3.1 Surface Chemistry and Morphology of CNTs

Fig. 2 shows the FTIR spectra of pristine and surface treated CNTs. There were no evident functional groups detected on the pristine CNT surface. After the attachment of surfactant molecules, several peaks at wave numbers 1100-1350 cm^{-1} , 1470-1520 cm^{-1}

and 2870-2950 cm^{-1} appeared, which correspond to C-O stretching vibration, aromatic =C-H and ring C=C stretching vibration, and -CH₃, -CH₂ stretching vibration, respectively. With more adsorption of surfactant on the CNT surface, the CNTs treated with 10 CMC presented more prominent intensive peaks in the spectra.

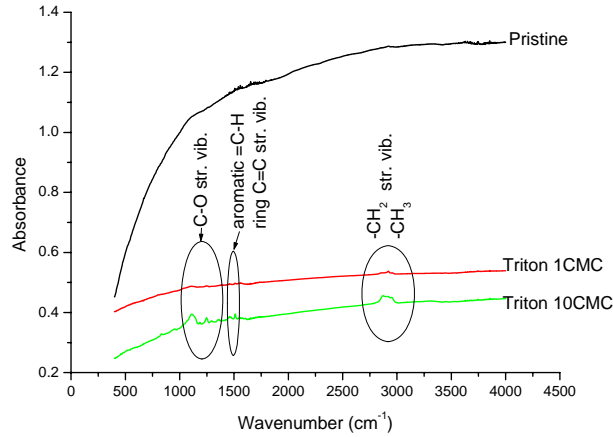


Fig. 2 FTIR spectra of CNTs with and without Triton treatment

Table 1 Intensities for D and G bands of CNTs

Conditions	Band intensity		I_D/I_G
	I_D (~1350 cm^{-1})	I_G (~1580 cm^{-1})	
Pristine	7372.20	8060.53	0.915
1 CMC treated	9740.82	10704.20	0.910
10 CMC treated	6475.66	7144.29	0.906

Raman spectroscopy was employed to verify whether the surfactant treatment resulted in physical adsorption rather than disturbing the CNT structure by inducing defects. It is well known that the two most prominent features of CNT in Raman spectra are the D and G bands appearing at the wave numbers of 1350 cm^{-1} and 1580 cm^{-1} . While the G band corresponds to the sound sp^2 carbon networks, the D band represents the disorder-induced character. The integrated intensity ratio of D and G bands, I_D/I_G , is often used to evaluate the defect density of CNT [19,20]. Table 1 gives the intensities for D and G bands of the CNTs with and without treatment. The I_D/I_G ratios for the three CNTs with different surface characteristics exhibited negligible variations, confirming that the surfactant treatment did not generate extra defects onto CNTs.

The typical morphologies of CNTs before and after ultrasonication in the presence of surfactant are shown in Fig. 3. It is clearly seen that the large agglomerates and closely packed CNTs are prevalent in the pristine state (Fig. 3a), which became significantly loosened after the surface treatment (Fig. 3b, c).

3.2 Thermomechanical properties

The storage modulus (G') and $\tan \delta$ curves of the nanocomposites obtained from the

DMA measurement are shown in Fig. 4. The glass transition temperatures (T_g) estimated from the peaks of $\tan \delta$ curves are plotted in Fig. 5. Both the T_g and the storage modulus at temperatures above T_g increased with increasing CNT content. The surfactant-treated CNT/epoxy nanocomposites exhibited much higher values than the untreated counterpart for the same CNT content. These observations are probably attributed to the formation of networks of well-dispersed surfactant-treated CNTs in the epoxy matrix, which can immobilize polymer chains at elevated temperatures [21].

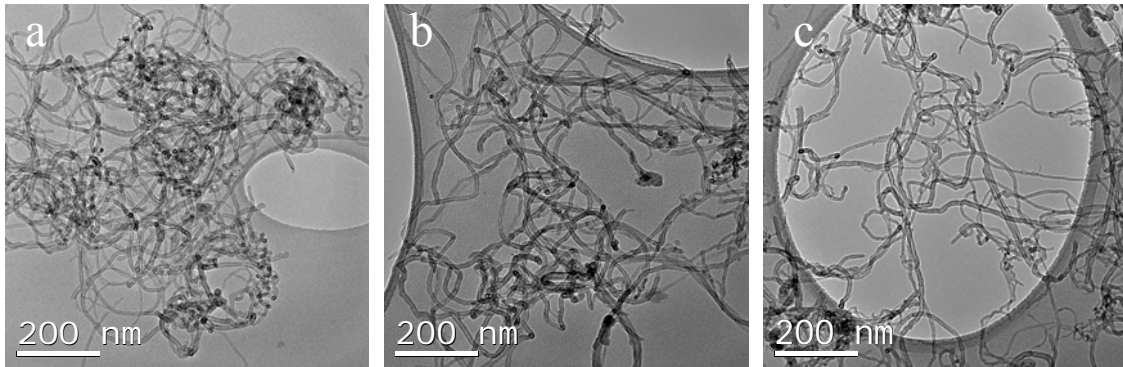


Fig. 3 TEM images of (a) pristine; (b) Triton X-100 (1 CMC) treated; and (c) Triton X-100 (10 CMC) treated CNTs

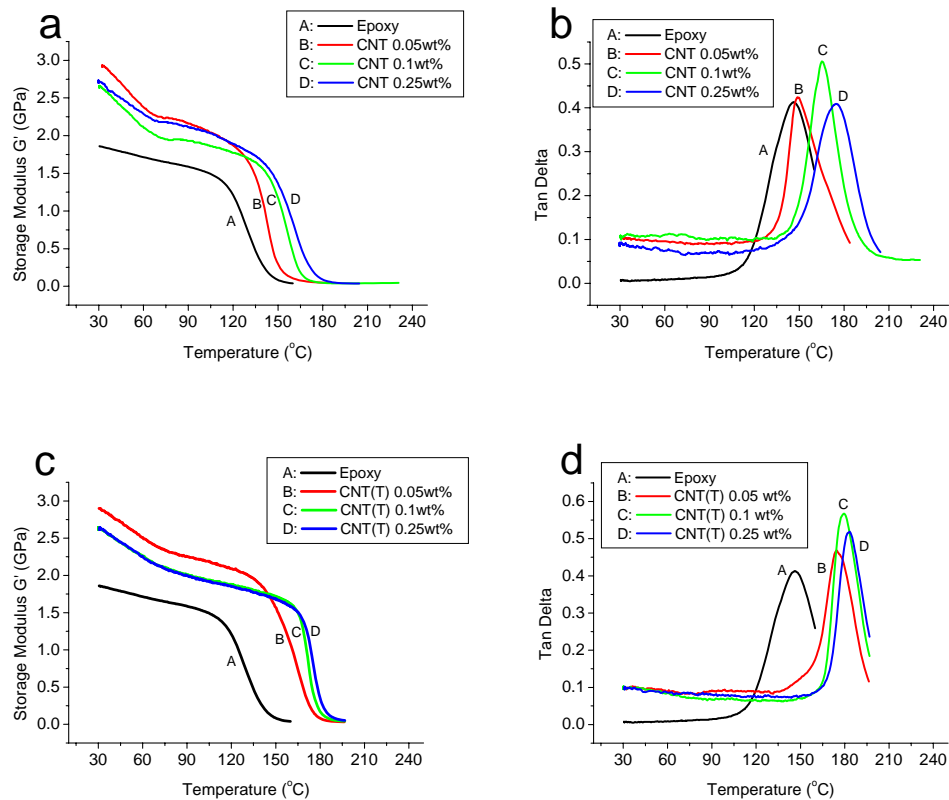


Fig. 4 (a) Storage modulus (G') and (b) $\tan \delta$ of pristine CNT/epoxy nanocomposites; (c) storage modulus (G') and (d) $\tan \delta$ of 10 CMC Triton treated CNT/epoxy nanocomposites as a function of temperature

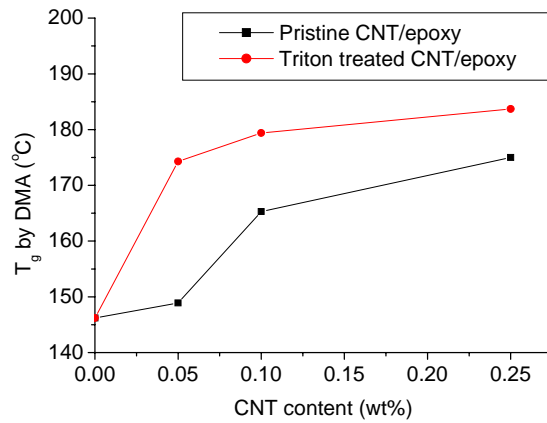


Fig. 5 Glass transition temperature (T_g) of CNT/epoxy nanocomposites

3.3 Mechanical properties

Fig. 6 shows the flexural properties of CNT/epoxy nanocomposites. With the increasing CNT content, both the flexural strength and modulus increased consistently. The surfactant treated CNT composites exhibited much better performances than those without treatment, which confirmed the ameliorating effects of the surface treatment on mechanical properties of the composites. Certainly, the CNT-matrix interfacial adhesion played an important role in determining these properties. Similar dependencies of mechanical properties of nanocomposites on interfacial adhesion of CNTs and graphite nanoparticles have been reported in many previous works [1, 22].

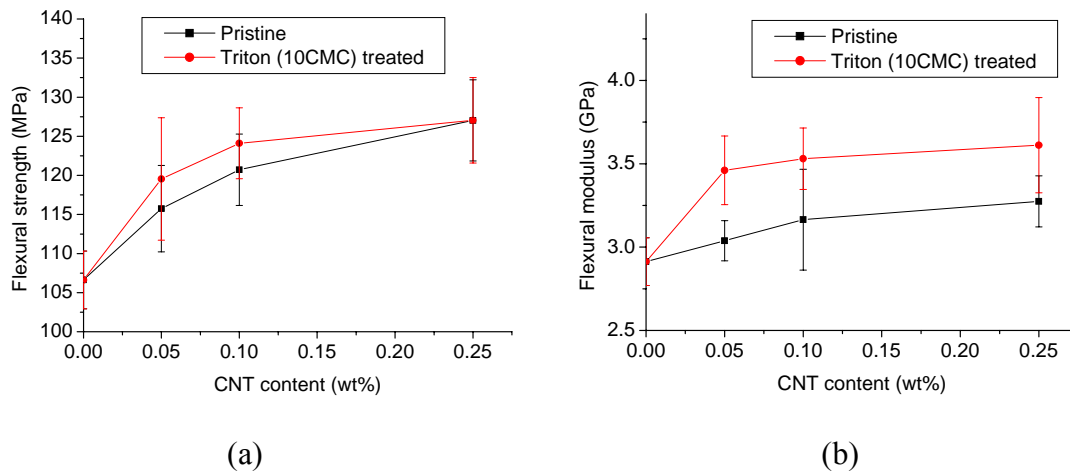


Fig. 6 (a) Flexural strength and (b) flexural modulus of CNT/epoxy nanocomposites with and without Triton (10 CMC) treatment

A significant improvement in impact strength was achieved with the addition of CNTs, especially after the Triton treatment, as shown in Fig. 7. It is remarkable to note that the improvement due to 0.25 wt% surfactant treated CNTs was about 60% compared to the neat epoxy (from 3.26 to 5.19 kJ/m²). The morphologies of impact fracture surfaces of the nanocomposites with CNT content of 0.1 wt% are presented in Fig. 8. There were

clear differences between the pristine and surfactant treated CNT nanocomposites: a smoother fracture surface with small-sized, repetitive spatulate patterns was seen for the former sample (Fig. 8a), while a rougher and more fluctuant morphology with large, elongated radial crack patterns was seen on the latter surface (Fig. 8c). Judging from the much higher impact fracture toughness of the nanocomposites containing surfactant-treated CNTs, the fracture surface morphology with elongated radial crack patterns corresponded to a higher crack growth resistance of the composites. However, it is not clear how the surfactant treatment gave rise to the elongated radial crack patterns on the fracture surface. Meanwhile, when examined at a high magnification, CNT agglomerates were observed on both fracture surfaces: scattered larger-size aggregations of pristine CNTs are seen (Fig. 8b), while some smaller and well-distributed aggregations are seen for the treated CNTs (Fig. 8d).

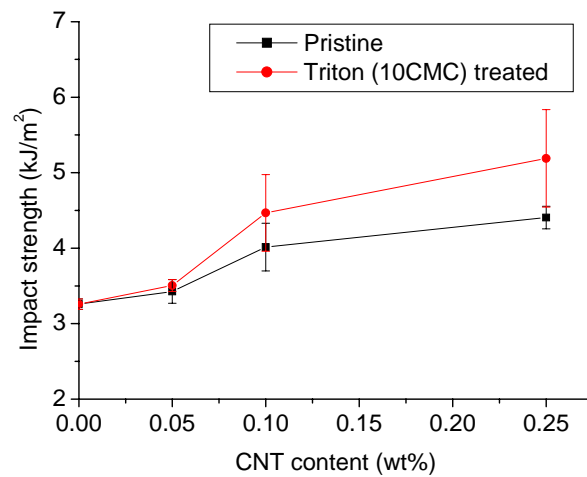
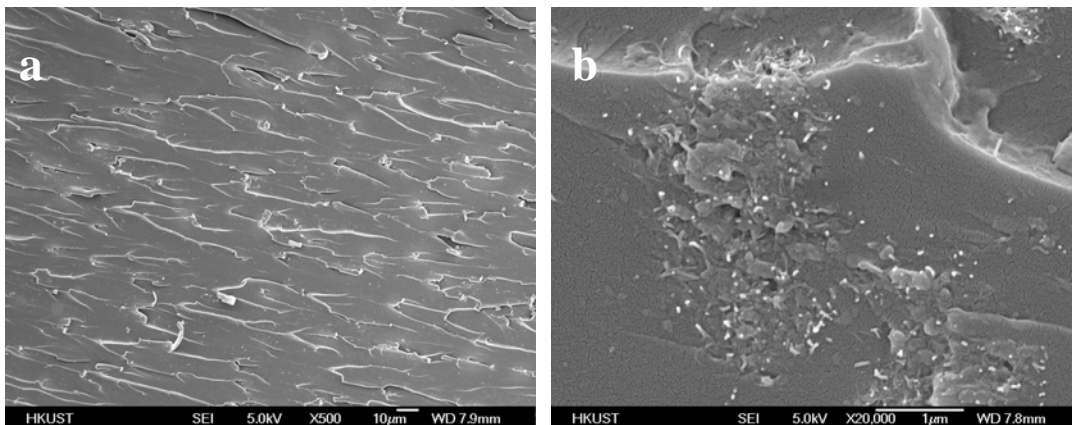


Fig. 7 Impact fracture toughness of CNT/epoxy nanocomposites with and without Triton (10 CMC) treatment



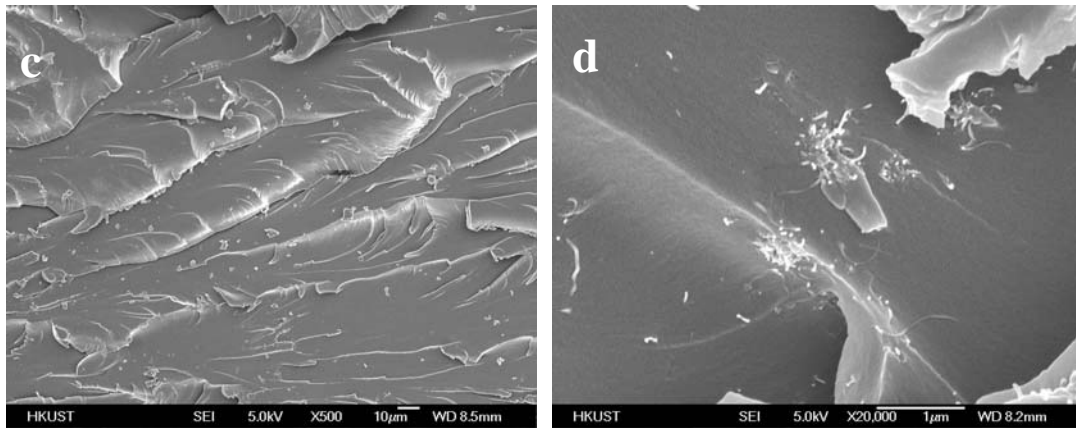


Fig. 8 SEM images of impact fracture surfaces of (a,b) pristine; (c,d) Triton (10 CMC) treated CNT/epoxy nanocomposites

3.4 Electrical conductivity

The electrical conductivities of CNT/epoxy nanocomposites were measured, as shown in Fig. 9. It is interesting to note that at a low CNT content (i.e. less than about 0.06 wt%), the electrical conductivity of the pristine CNT nanocomposites was higher than the composites containing surfactant treated CNTs. However, with further increasing the CNT content, the surfactant exhibited ameliorating effects on improving CNT dispersion with better formation of conductive networks within the polymer matrix, thus leading to significant increase in the electrical conductivity of composites, especially at CNT contents of 0.075 to 0.1wt%, just above the percolation threshold. The change in the CMC concentration did not alter much the electrical conducting behaviour.

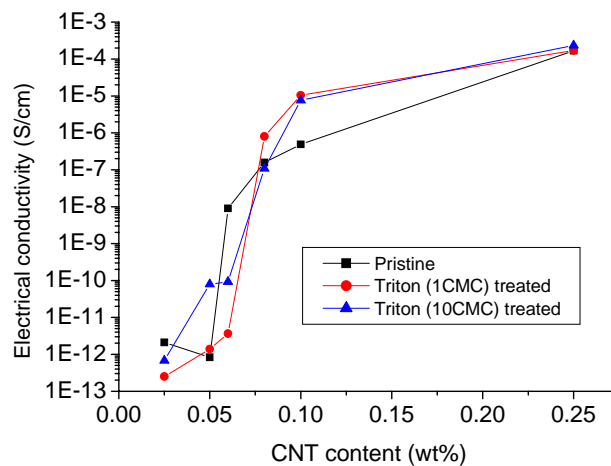


Fig. 9 Electrical conductivity of CNT/epoxy nanocomposites with and without Triton treatment.

4. CONCLUSIONS

The effects of surfactant treatment of CNTs on the mechanical and functional properties of CNT/epoxy nanocomposites were studied. The enhanced uniformity of CNT

distribution assisted by surfactant played an important role in improving the mechanical, thermomechanical and electrical properties of CNT/epoxy nanocomposites. The concomitant improvement in dispersion of CNTs in the matrix was also beneficial to the formation of electrical networks.

REFERENCES

- 1- Ma P.C., Kim J.K., Tang B.Z., "Effects of silane functionalization on the properties of carbon nanotube/epoxy nanocomposites", *Composites Science and Technology*, 2007;67:2965-2972.
- 2- Lanticse L.J., Tanabe Y., Matsui K., Kaburagi Y., Suda K., Hoteida M., Endo M., Yasuda E., "Shear-induced preferential alignment of carbon nanotubes resulted in anisotropic electrical conductivity of polymer composites", *Carbon*, 2006;44:3078-3086.
- 3- Ryan K.P., Cadek M., Nicolosi V., Blond D., Ruether M., Armstrong G., Swan H., Fonseca A., Nagy J.B., Maser W.K., Blau W.J., Coleman J.N., "Carbon nanotubes for reinforcement of plastics? A case study with poly(vinyl alcohol)", *Composites Science and Technology*, 2007;67:1640-1649.
- 4- Lourie O, Cox D.E., Wagner H.D., "Buckling and collapse of embedded carbon nanotubes" *Physical Review Letters* 1998;81:1638-1641.
- 5- Thess A., Lee R., Nikolaev P., Dai H., Petit P., Robert J., Xu C., Lee Y.H., Kim S.G., Rinzler A.G., Colbert D.T., Scuseria G.E., Tomanek D., Fischer J.E., Smalley R.E., "Crystalline ropes of metallic carbon nanotubes", *Science*, 1996;273:483-487.
- 6- Park K.C., Hayashi T., Tomiyasu H., Endo M., Dresselhaus M.S., "Progressive and invasive functionalization of carbon nanotubes sidewalls by diluted nitric acid under supercritical conditions", *Journal of Materials Chemistry*, 2005;15:407-411.
- 7- Kim Y.J., Shin T.S., Choi H.D., Kwon J.H., Chung Y., Yoon H.G., "Electrical conductivity of chemically modified multiwalled carbon nanotube/epoxy composites", *Carbon*, 2005;43:23-30.
- 8- Sham M.L., Kim J.K., "Surface functionalities of multi-wall carbon nanotubes after UV/ozone and TETA treatments", *Carbon*, 2006;44:768-777.
- 9- Seo M., Park S., Lee S., "Influence of atmospheric plasma on physicochemical properties of vapor-grown graphite nanofibers", *Journal of Colloid and Interface Science*, 2005;285:306-313.
- 10- Gabriel G., Sauthier G., Fraxedas J., Moreno-Manas M., Martínez M.T., Miravittles C., Casabó J., "Preparation and characterization of single-walled carbon nanotubes functionalized with amines", *Carbon*, 2006;44:1891-1897.
- 11- Ma P.C., Kim J.K., Tang B.Z., "Functionalization of carbon nanotubes using a silane coupling agent", *Carbon*, 2006;44:3232-3238.
- 12- Lee Y.S., Cho T.H., Lee B.K., Rho J.S., An K.H., Lee Y.H., "Surface properties of fluorinated single-walled carbon nanotubes", *Journal of Fluorine Chemistry*, 2003;120:99-104.
- 13- Gong X., Liu J., Baskaran S., Voise R.D., Young J.S., "Surfactant-assisted processing of carbon nanotube/polymer composites", *Chemistry of Materials*,

- 2000;12:1049-1052.
- 14- Grossiord N., Loos J., Regev O., Koning C.E., "Toolbox for dispersing carbon nanotubes into polymers to get conductive nanocomposites", *Chemistry of Materials*, 2006;18:1089-1099.
 - 15- Vaisman L., Marom G., Wagner H.D., "Dispersions of surface-modified carbon nanotubes in water-soluble and water-insoluble polymers", *Advance Functional Materials*, 2006;16:357-363.
 - 16- Kim T.H., Doe C., Kline S.R., Choi S., "Water-redispersible isolated single-walled carbon nanotubes fabricated by in situ polymerization of micelles", *Advanced Materials*, 2007;19:929-933.
 - 17- Vaisman L., Wagner H.D., Marom G., "The role of surfactants in dispersion of carbon nanotubes", *Advances in Colloid and Interface Science*, 2006;128-130:37-46.
 - 18- Barbero M.C., Valpuesta J.M., Rial E., Gurtubay J.I.G., Goñi F.M., Macarulla J.M., "Effect of the nonionic detergent Triton X-100 on mitochondrial succinate-oxidizing enzymes", *Archives of Biochemistry and Biophysics*, 1984;228:560-568.
 - 19- Tuinstra F., Koenig J.L., "Raman spectrum of graphite", *Journal of chemical physics*, 1970;53:1126-1130.
 - 20- Sood A.K., Gupta R., Asher S.A., "Origin of the unusual dependence of Raman D band on excitation wavelength in graphite-like materials", *Journal of Applied Physics*, 2001;90:4494-4497.
 - 21- Ogasawara T., Ishida Y., Ishikawa T., Yokota R., "Characterization of multi-walled carbon nanotube/phenylethynyl terminated polyimide composites", *Composites Part A*, 2004;35:67-74.
 - 22- Li J., Kim J.K., Sham M.L., Marom G., "Morphology and properties of UV/Ozone treated graphite nanoplatelet/epoxy nanocomposites", *Composite Science Technology*, 2007;67:296-305.